5,10-linked naphthodithiophenes as the building block for semiconducting polymers

Itaru Osaka[1,2]**, Koki Komatsu**[2]**, Tomoyuki Koganezawa**[3] **and Kazuo Takimiya**[1,2]

[1] Emergent Molecular Function Research Group, Center for Emergent Matter Science, RIKEN, 2-1 Hirosawa, Wako, Saitama 351-0198, Japan
[2] Department of Applied Chemistry, Graduate School of Engineering, Hiroshima University, 1-4-1 Kagamiyama, Higashi-Hiroshima, Hiroshima 739-8527, Japan
[3] Japan Synchrotron Radiation Research Institute, Sayo-gun, Hyogo 679-5198, Japan

E-mail: itaru.osaka@riken.jp and takimiya@riken.jp

Abstract

We present new semiconducting polymers incorporating naphtho[1, 2-*b*:5, 6-*b'*] dithiophene (NDT3) and naphtho[2, 1-*b*:6, 5-*b'*] dithiophene (NDT4), which are linked at the naphthalene positions, in the polymer backbone. It is interesting that the trend in the ordering structure and thus charge transport properties are quite different from what were observed in the isomeric polymers where the NDT3 and NDT4 cores are linked at the thiophene α-positions. In the thiophene-linked NDT system, the NDT3-based polymer (PNDT3BT) gave the better ordering in thin films and thus the high charge carrier mobility compared to the NDT4-based polymer (PNDT4BT). In the meantime, in the naphthalene-linked NDT system, the NDT4-based polymer (PNDT4iBT) provided the superior properties. Considering that PNDT4iBT has relatively low highest occupied molecular orbital (HOMO) energy level (−5.2 eV) and moderately high mobilities in the order of 10^{-2} cm^2 V^{-1} s^{-1}, the NDT4 core, when linked at the naphthalene positions, can be a good building unit for the development of high-performance semiconducting polymers for both organic field-effect transistors and photovoltaic devices.

S Online supplementary data available from stacks.iop.org/STAM/15/024201/mmedia

Keywords: semiconducting polymers, naphthodithiophene, organic field-effect transistors

1. Introduction

With the excellent solution processability, film uniformity, and thermal stability, semiconducting polymers are fascinating materials for solution-processed devices such as organic field-effect transistors (OFETs) and organic photovoltaic devices (OPVs) [1, 2]. In the past few decades, a number of semiconducting polymers have been reported and the performances of those based devices have greatly improved. In the development of semiconducting polymers, exploration of thiophene-based fused heteroaromatic rings used as the building unit is one of the most important steps, since they determine the electronic and ordering structures of the polymers. Such units include thienothiophene [3, 4], benzodithiophene [5–7], dithienothiophene [8], and tetrathienoacene [9]. It should also be noted that the incorporation manner of the building units in the backbone significantly affects the above-mentioned polymer properties [1, 2, 10].
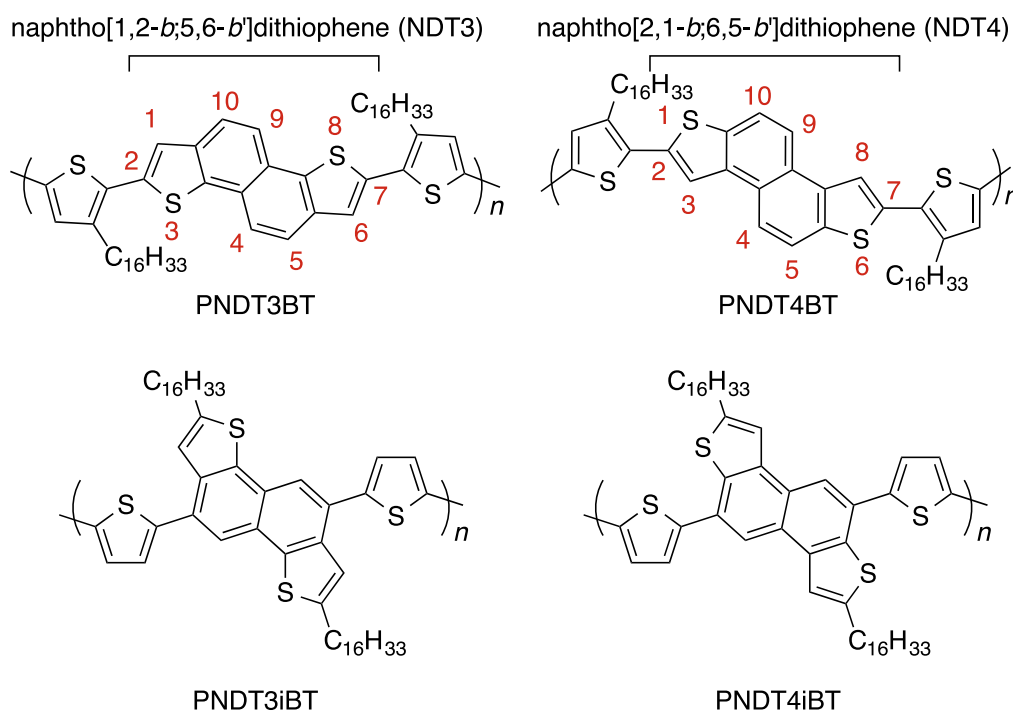
Figure 1. Chemical structures of semiconducting polymers consisting of NDT3 or NDT4 with bithiophene: previously reported NDT-based polymers, where the NDT cores are linked at the thiophene *α*-positions (2, 7-) positions (top), and newly synthesized polymers, where the NDT cores are linked at the naphthalene (5, 10-) positions (bottom).

Recently, we have reported on the synthesis, characterization, and OFET and OPV applications of a series of semiconducting polymers based on naphthodithiophenes (NDTs), four-ring-fused heteroaromatic system (figure 1) [11–15]. Among the four different NDT isomers which can be selectively synthesized, angular shaped naphtho[1, 2-*b*:5, 6-*b*′]dithiophene (NDT3) and naphtho[2, 1-*b*:6, 5-*b*′]dithiophene (NDT4) afforded both good electronic structures and ordering structures when they are linked at the *α*-positions of the thiophene substructure, in which the molecular long axis is parallel to the polymer backbone [12]. More recently, while other groups independently reported on the synthesis of 4, 9- and 5, 10-functionalized NDT3 and the corresponding semiconducting materials [16–19], we have successfully introduced various functional groups including the boronic acid ester group at the 5, 10-positions [20]. This allowed us to produce a polymer with NDT3 linked at the corresponding positions. Herein, we study the effect of the linking position in NDT3- and NDT4-based semiconducting polymers (figure 1) in terms of electronic structure, ordering structure, and OFET performances.

2. Experimental details

2.1. Materials

2, 7-di(hexadecyl)naphtho[1, 2-*b*:5, 6-*b*′]dithiophene (**1**) [21] and 2, 7-di(hexadecyl)naphtho[2, 1-*b*:6, 5-*b*′]dithiophene (**2**) [22] were synthesized according to the literature procedure. All chemicals are of reagent grade unless otherwise indicated.

All solvents were distilled prior to use. Polymerization was carried out with a microwave reactor (Biotage Initiator). Molecular weights were determined by gel permeation chromatography (GPC) with a TOSOH HLC-8121GPC/HT at 140 °C using *o*-dichlorobenzene (DCB) as a solvent and calibrated with polystyrene standards.

2.2. Synthesis

2.2.1. 2, 2′- (2, 7-dihexadecylnaphtho [1, 2-b:5, 6-b′] dithiophene-5, 10-diyl) bis(4, 4, 5, 5-tetramethyl-1, 3, 2-dioxaborolane) (3). Under nitrogen atmosphere, (1, 5-cyclooctadiene)(methoxy)iridium (I) dimer (10 mg, 0.05 mmol) and 4, 4′-di-*tert*-butyl-2, 2′-di-pyridyl (8 mg, 0.1 mmol) were dissolved in dry cyclohexane (10 mL). Bis(pinacolate)diborane (168 mg, 0.66 mmol) and **1** (207 mg, 0.3 mmol) was then added to the mixture, and refluxed for 12 h. The reaction mixture was poured into water and the resulting mixture was extracted with chloroform. The combined organic layer was washed with water and brine, and dried by MgSO$_4$. After removal of the solvent under reduced pressure, the residue was purified by column chromatography on silica gel eluted with chloroform (R_f = 0.4) to give **3** as white solids (255 g, 90%). Proton nuclear magnetic resonance (^{1}H-NMR, 400 MHz, CDCl$_3$): δ (s, 2 H), 7.74 (s, 2 H), 3.01 (t, J = 7.4 Hz, 4 H), 1.83-1.20 (m, 80 H), 0.88 (t, J = 7.0 Hz, 6 H). ^{13}C-NMR (400 MHz, CDCl$_3$): δ 145.6, 140.8, 137.9, 130.2, 126.6, 123.7, 84,1, 32.1, 31.9, 31.2, 29.9, 29.8, 29.8, 29.8, 29.6, 29.5, 29.5, 25.2, 22.9, 14.3. Elemental analysis calculated for C$_{58}$H$_{94}$B$_2$O$_4$S$_2$: C, 74.02; H, 10.07. Found: C, 74.14; H, 10.35.

2.2.2. 2, 2′- (2, 7-dihexadecylnaphtho [2, 1-b:6, 5-b′] dithiophene-5, 10-diyl) bis(4, 4, 5, 5-tetramethyl-1, 3, 2-dioxaborolane) (4). Under nitrogen atmosphere, (1, 5-cyclooctadiene) (methoxy)iridium (I) dimer (179 mg, 0.27 mmol) and 4, 4′-di-*tert*-butyl-2, 2′-di-pyridyl (145 mg, 0.54 mmol) were dissolved in dry cyclohexane (50 mL). Bis(pinacolate)diborane (3.02 g, 11.9 mmol) and **2** (3.73 g, 5.41 mmol) was then added to the mixture, and refluxed for 12 h. The reaction mixture was poured into water and the resulting mixture was extracted with chloroform. The combined organic layer was washed with water and brine, and dried by MgSO$_4$. After removal of the solvent under reduced pressure, the residue was purified by column chromatography on silica gel eluted with chloroform ($R_f = 0.4$) to give **3** as white solids (4.57 g, 90%). ^{1}H-NMR (400 MHz, CDCl$_3$): δ (s, 2 H), 7.82 (s, 2 H), 3.01 (t, $J = 7.4$ Hz, 4 H), 1.83-1.20 (m, 80 H), 0.88 (t, $J = 7.0$ Hz, 6 H). ^{13}C-NMR (400 MHz, CDCl$_3$): δ 147.8, 140.3, 137.0, 128.5, 127.2, 119.0, 84.4, 32.1, 31.9, 31.2, 29.8, 29.7, 29.6, 29.5, 25.1, 22.8, 14.3. Elemental analysis calculated for C$_{58}$H$_{94}$B$_2$O$_4$S$_2$: C, 74.02; H, 10.07. Found: C, 74.14; H, 10.35.

2.2.3. PNDT3iBT. Under nitrogen atmosphere, **3** (94.1 mg, 0.1 mmol), 5, 5′-dibromo-2, 2′-bithiophene (32.4 mg, 0.1 mmol), potassium carbonate aqueous solution (4 mL, 2 M), 1 drop of Aliquat 336, and toluene (6 mL) were added in a reaction vial. The mixture was purged with argon for 30 min, and then dichlorobis(triphenylphosphine)palladium (II) (3.5 mg, 0.005 mol) was added and sealed. The vial was subjected to a microwave reactor, and heated at 100 °C for 2 h. After cooling to 40 °C, a toluene solution of phenyl boronic acid was added, and the vial was further heated in a microwave reactor at 100 °C for 30 min. The reaction mixture was then poured into acetic acid and extracted with chloroform. The organic layer was washed with water, and was poured into methanol (100 mL) containing 10 mL of 2 M hydrochloric acid. The precipitate was collected, washed sequentially with methanol, hexane, and chloroform with Soxhlet extraction apparatus, and then collected with chlorobenzene. The solvent was removed under reduced pressure and the residue was reprecipitated in methanol. The polymer was collected by filtration and dried in a vacuum (red solids, 152 mg, 89%). $M_n = 667\,00$, $M_w = 197\,300$.

2.2.4. PNDT4iBT. Under nitrogen atmosphere, **4** (94.1 mg, 0.1 mmol), 5, 5′-dibromo-2, 2′-bithiophene (32.4 mg, 0.1 mmol), potassium carbonate aqueous solution (4 mL, 2 M), 1 drop of Aliquat 336, and toluene (6 mL) were added in a reaction vial. The mixture was purged with argon for 30 min, and then dichlorobis(triphenylphosphine)palladium (II) (3.5 mg, 0.005 mol) was added and sealed. The vial was subjected to a microwave reactor, and heated at 100 °C for 2 h. After cooling to 40 °C, a toluene solution of phenyl boronic acid was added, and the vial was further heated in a microwave reactor at 100 °C for 30 min. The reaction mixture was then poured into acetic acid and extracted with chloroform. The organic layer was washed with water, and

was poured into methanol (100 mL) containing 10 mL of 2 M hydrochloric acid. The precipitate was collected, was washed sequentially with methanol, hexane, and chloroform with Soxhlet extraction apparatus, and then collected with chlorobenzene. The solvent was removed under reduced pressure and the residue was reprecipitated in methanol. The polymer was collected by filtration and dried in a vacuum (red solids, 130 mg, 76%). $M_n = 260\,00$, $M_w = 523\,00$.

2.3. Instrumentation

Cyclic voltammograms of the polymer films were recorded on a BAS electrochemical analyzer, model 612D, in acetonitrile containing tetrabutylammonium hexafluorophosphate (Bu$_4$NPF$_6$, 0.1 M) as supporting electrolyte at a scan rate of 100 mV s^{-1}. Counter and working electrodes were made of Pt, and the reference electrode was Ag/AgCl. All the potentials were calibrated with the standard ferrocene/ferrocenium redox couple (Fc/Fc$^+$: E$_{1/2}$ = +0.43 V measured under identical conditions). The photoelectron spectra were measured using a spectrometer model AC-2 (Riken Keiki Co., Ltd). UV−vis absorption spectra were measured using a Shimadzu UV-3600 spectrometer. Dynamic force-mode atomic force microscopy study was carried out on a Nanocute scanning probe microscope system (SII Nanotechnology, Inc.). Grazing incidence x-ray diffraction (GIXD) experiments were conducted at the SPring-8 on beamline BL19B2. The sample was irradiated at a fixed incident angle on the order of 0.12° through a Huber diffractometer with an x-ray energy of 12.39 keV ($\lambda = 1$ Å), and the GIXD patterns were recorded with a 2D image detector (Pilatus 300 K). Samples for the x-ray measurements were prepared by casting the polymer solution on the 1*H*, 1*H*, 2*H*, 2*H*-perfluorodecyltriethoxysilane (FDTS)-modified Si/SiO$_2$ substrate.

2.4. OFET fabrication and measurements

All film fabrication processes except substrate cleaning were performed in a glove box. Heavily doped n$^+$-Si (100) wafers with 200-nm-thick thermally grown SiO$_2$ ($C_i = 17.3$ nF cm^{-2}) were used for the substrate. The Si/SiO$_2$ substrates were ultrasonicated with acetone and isopropanol for 10 min, respectively, and then were subjected to UV-ozone treatment for 20 min. The cleaned substrates were treated with FDTS to form a self-assembled monolayer, in which the wafers were exposed to FDTS vapor in a closed desiccator. Polymer layers were then spin-coated from hot (~100 °C) 3 g L^{-1} DCB solution at 1000 rpm for 10 s and then 2500 rpm for 35 s, and subsequently annealed at 150 °C for 30 min, respectively, under nitrogen. On top of the polymer thin films, Au drain and source electrodes (thickness 80 nm) were deposited in a vacuum through a shadow mask, where the drain−source channel length (*L*) and width (*W*) are 40 μm and 3.0 mm, respectively.

Current−voltage characteristics of the OFET devices were measured at room temperature in air with a Keithley 4200-SCS semiconductor characterization system. Field-effect mobilities were calculated in the saturation regime

Scheme 1. Synthetic route to PNDT3iBT and PNDT4iBT.
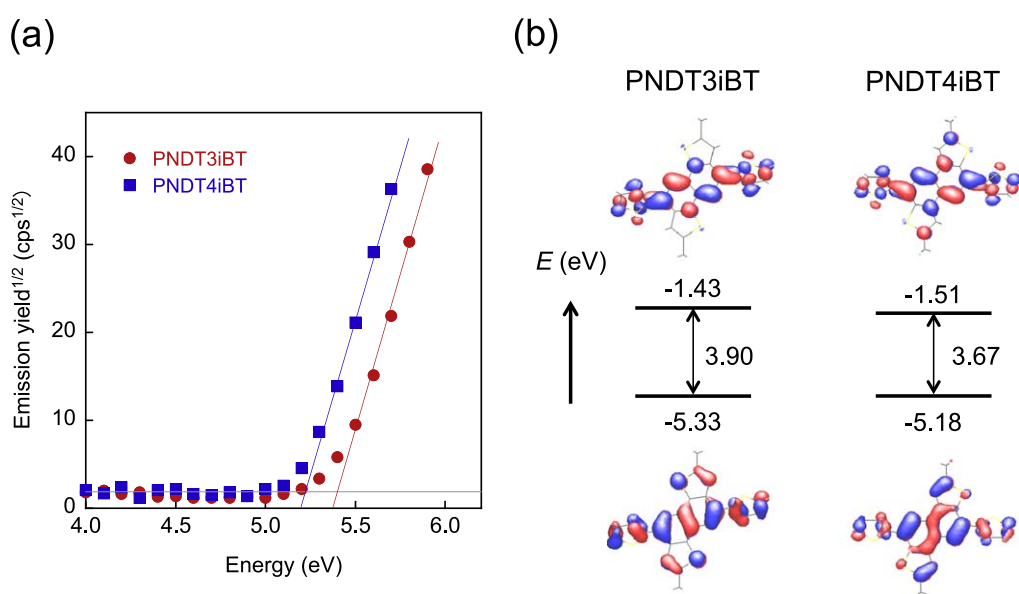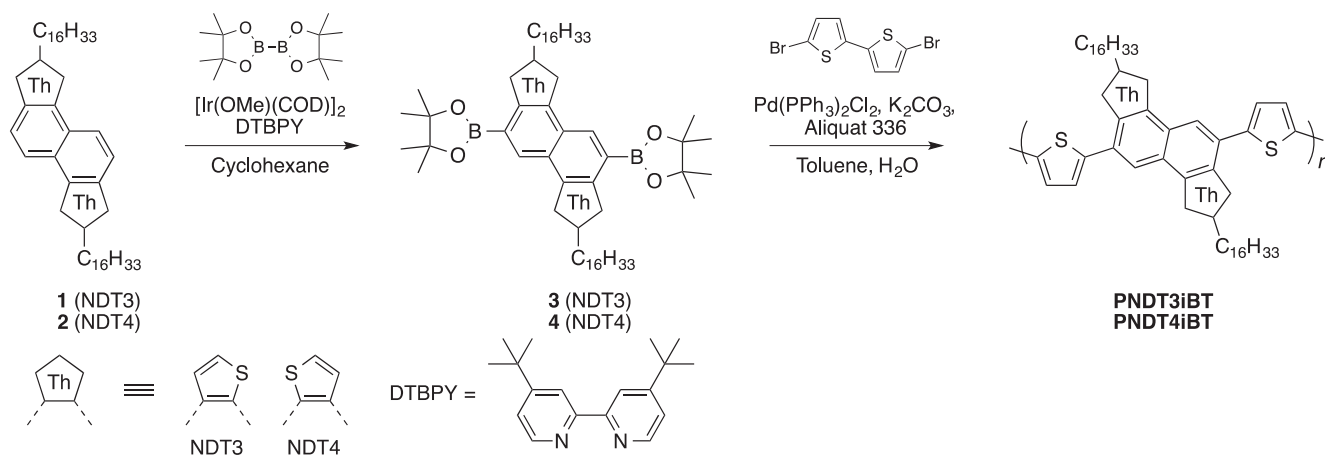
Figure 2. (a) Photoelectron spectra of the polymer thin films. (b) Highest occupied and lowest unoccupied molecular orbitals (HOMOs and LUMOs) and their energy levels in the model compounds calculated by time-dependent DFT methods at the B3LYP/6-31(d) level.

Table 1. Polymer properties.

Polymer	M_n (kDa)[b]	M_w (kDa)[b]	E_H (eV)[c]	E_g (eV)[d]	λ_{max} (nm)[e] solution	λ_{max} (nm)[e] film	$d\pi$ (Å)[f]	μ_h (cm^2 V^{-1} s^{-1})[g]
PNDT3iBT	66.7	197.3	−5.37	2.33	461	453	3.9	~0.0023
PNDT4iBT	26.0	52.3	−5.22	2.17	491	503	3.7	~0.011
PNDT3BT[a]	28.9	45.8	−5.00	2.15	506, 540	504, 539	3.6	~0.77
PNDT4BT[a]	29.5	46.5	−5.10	2.24	492, 529	491, 528	3.6	~0.19

[a] From [12].
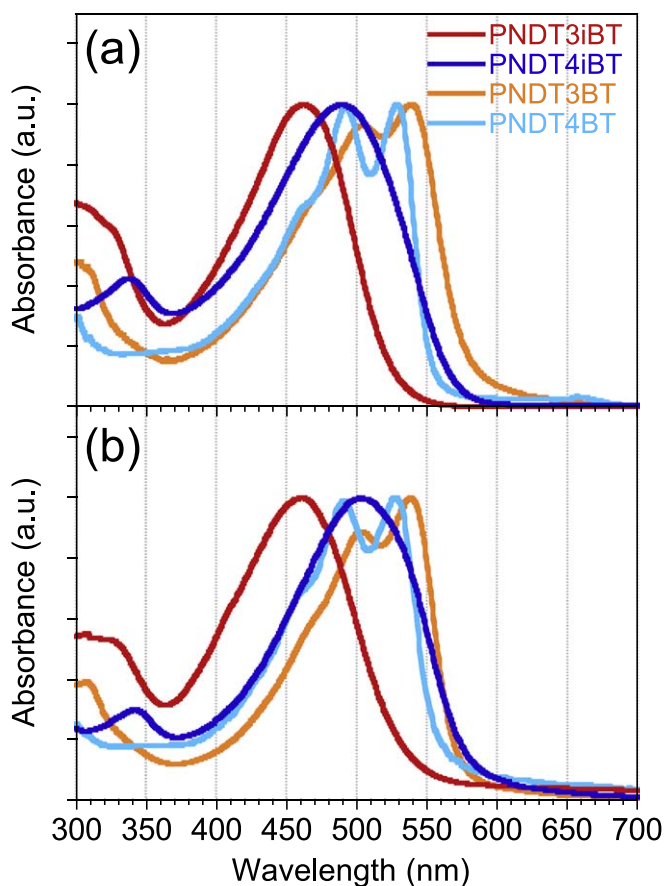[b] Determined by high-temperature GPC (140 °C), calibrated with polystyrene standard.
[c] HOMO energy levels estimated by the photoelectron spectroscopy.
[d] Optical bandgaps estimated from the onset of the film absorption spectra.
[e] Absorption maxima.
[f] π–π stacking distance.
[g] Hole mobilities.

Figure 3. UV–vis absorption spectra of PNDT3iBT, PNDT4iBT, PNDT3BT, and PNDT4BT in the chlorobenzene solution (a) and in the film (b).
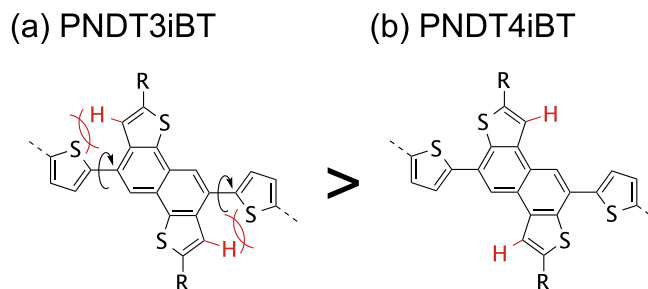

Figure 4. Difference of the steric hindrance between the NDT core and the thiophene rings. (a) PNDT3iBT, (b) PNDT4iBT.

revealed by the differential scanning calorimetry (DSC, figure S7).

Highest occupied molecular orbital (HOMO) energy levels (E_H) of the polymers were evaluated in film samples with the photoelectron spectroscopy in air (PESA, figure 2(a)). It is interesting to note that while in the present naphthalene-linked NDT system (PNDTiBTs) the NDT3-polymer (PNDT3iBT) gives lower E_H (−5.37 eV) than the NDT4-polymer (PNDT4iBTs) (−5.22 eV), in the thiophene-linked NDT system (PNDTBTs) the NDT4-polymer (PNDT4BT) gives lower E_H (−5.10 eV) than the NDT3-polymer (PNDT3BT) (−5.00 eV) (table 1). The trend of E_H in PNDTiBTs is consistent with the computation (figure 2(b)). The lower E_H in PNDT3iBT compared to PNDT4iBT is related to the wider bandgap of PNDT3iBT (*vide infra*).

Figure 3 shows the ultraviolet-visible (UV–vis) absorption spectra of PNDT3iBT and PNDT4iBT, together with PNDT3BT and PNDT4BT, in the chlorobenzene solution (figure 3(a)) and the film (figure 3(b)). PNDTiBTs provided absorption maxima (λ_{max}) in the shorter wavelength region as compared to PNDTBTs, indicating that the effective π-conjugation is somewhat limited. This blue shift, as well as the lower lying E_H, in PNDTiBTs as compared to PNDTBTs is most likely due to the difference of the π-electron system of the NDT unit involved in the backbone; the whole NDT unit is involved for PNDTBTs, whereas only the naphthalene substructure for PNDTiBTs. In addition, the phenyl-thiophene linkage has some twist compared to the thiophene-thiophene linkage, giving rise to the limitation of effective π-conjugation length. It is interesting that the trend of the shift of λ_{max} was quite different between PNDTBTs and PNDTiBTs. While in PNDTBTs, the NDT3-based polymer (PNDT3BT; 506 and 540 nm) afforded λ_{max} at the longer wavelength region than the NDT4-based polymer (PNDT4BT; 492 and 529 nm) in the solution [12], in PNDTiBTs, the NDT4-based polymer (PNDT4iBT; 491 nm) gave λ_{max} at the longer region than the NDT3-based polymer (PNDT3iBT; 461 nm) (figure 3(a), table 1). This contrasting shift of λ_{max} between the NDT3 and NDT4 system in PNDTiBTs compared to PNDTBTs can be explained as follows. In PNDTiBTs, the β-hydrogens of the thiophene substructure in NDT3 head outside of the core in PNDT3iBT, which causes a steric hindrance between the β-hydrogens on the neighboring thiophene rings, leading to the limited π-conjugation. However, the β-hydrogens in NDT4 head inside

($V_D = −60$ V) of the I_D using the following equation,

$$I_D = (WC_i/2L)\,\mu\,(V_G − V_T)^2$$

where C_i is the capacitance of the dielectric layer, I_D is the source–drain current, and V_D, V_G, and V_T are the source-drain, gate, and threshold voltages, respectively. Current on/off ratios (I_{on}/I_{off}) were determined from the minimum current around $V_G = 0$–20 V (I_{off}) and the current at $V_G = −80$ V (I_{on}). The mobility data were collected from more than 10 different devices.

3. Results and discussion

Scheme 1 shows the synthetic route to PNDT3iBT and PNDT4iBT. Dialkyl-NDT3 (**1**) and -NDT4 (**2**) were borylated using an Ir catalyst to give **3** and **4**, respectively [23], which were then polymerized with dibromobithiophene via the Suzuki–Miyaura cross-coupling reaction, giving the corresponding polymers (PNDT3iBT and PNDT4iBT) in reasonable yields. The number and weight average molecular weight (M_n and M_w) of the polymers are summarized in table 1; $M_n = 66.7$ kDa and $M_w = 197.3$ kDa for PNDT3iBT and $M_n = 26.0$ kDa and $M_w = 52.3$ kDa for PNDT4iBT. Both polymers were soluble in warm chlorinated benzenes. Both the polymers are found to be thermally stable below 350 °C as
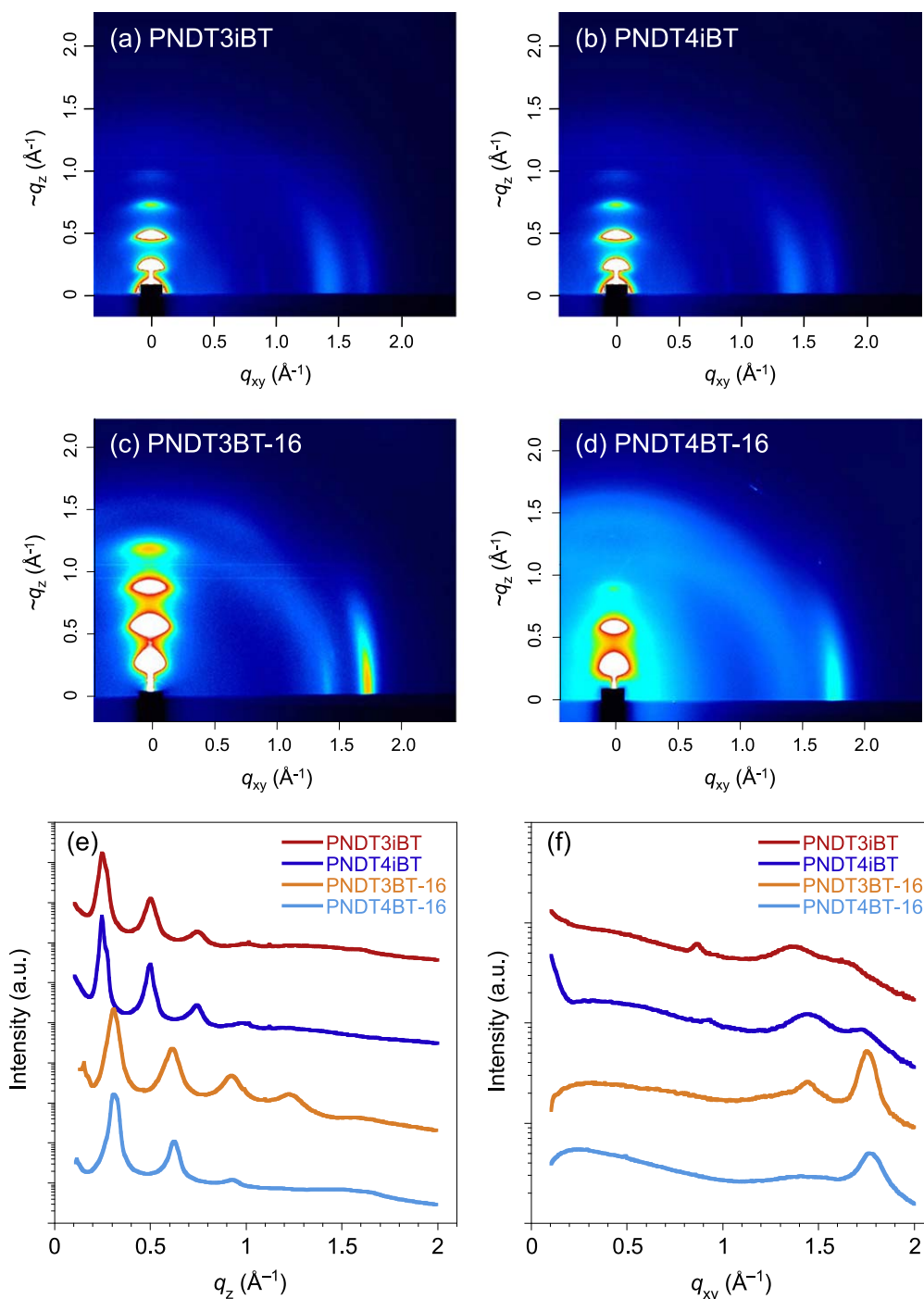
Figure 5. 2D-GIXD images of the PNDT3iBT (a), PNDT4iBT (b), PNDT3BT-16 (c), and PNDT4BT-16 (d) thin films, and their cross-sections along the q_z (e) and q_{xy} axes (f).

the core in PNDT4iBT, resulting in the reduced steric hindrance and thus a more coplanar backbone (figure 4). Density functional theory (DFT) calculation revealed that the dihedral angle between the naphthalene substructure of NDTs and the thiophene ring for PNDT4iBT (45.6°) was slightly smaller than for PNDT3iBT (47.6°), though the difference was very small, which is consistent with what was observed in the absorption spectra of the actual polymer system. Meanwhile, in PNDTBTs, PNDT4BT has a more zigzag shaped backbone than PNDT3BT and thus more likely to have conformational

defects in the backbone, giving rise to the slight limitation of π-conjugation in PNDT4BT, as we have reported.

The difference in λ_{max} between PNDT3iBT and PNDT4iBT was more prominent in the film absorption spectra (figure 3(b)), in which λ_{max} was 453 nm for PNDT3iBT and 503 nm for PNDT4iBT. This suggests that the PNDT4iBT backbone is more coplanar and therefore can pack more closely than the PNDT3iBT backbone. Notably, although λ_{max} of PNDT4iBT (the more red-shifted one in PNDTiBTs) is still located at the shorter wavelength region
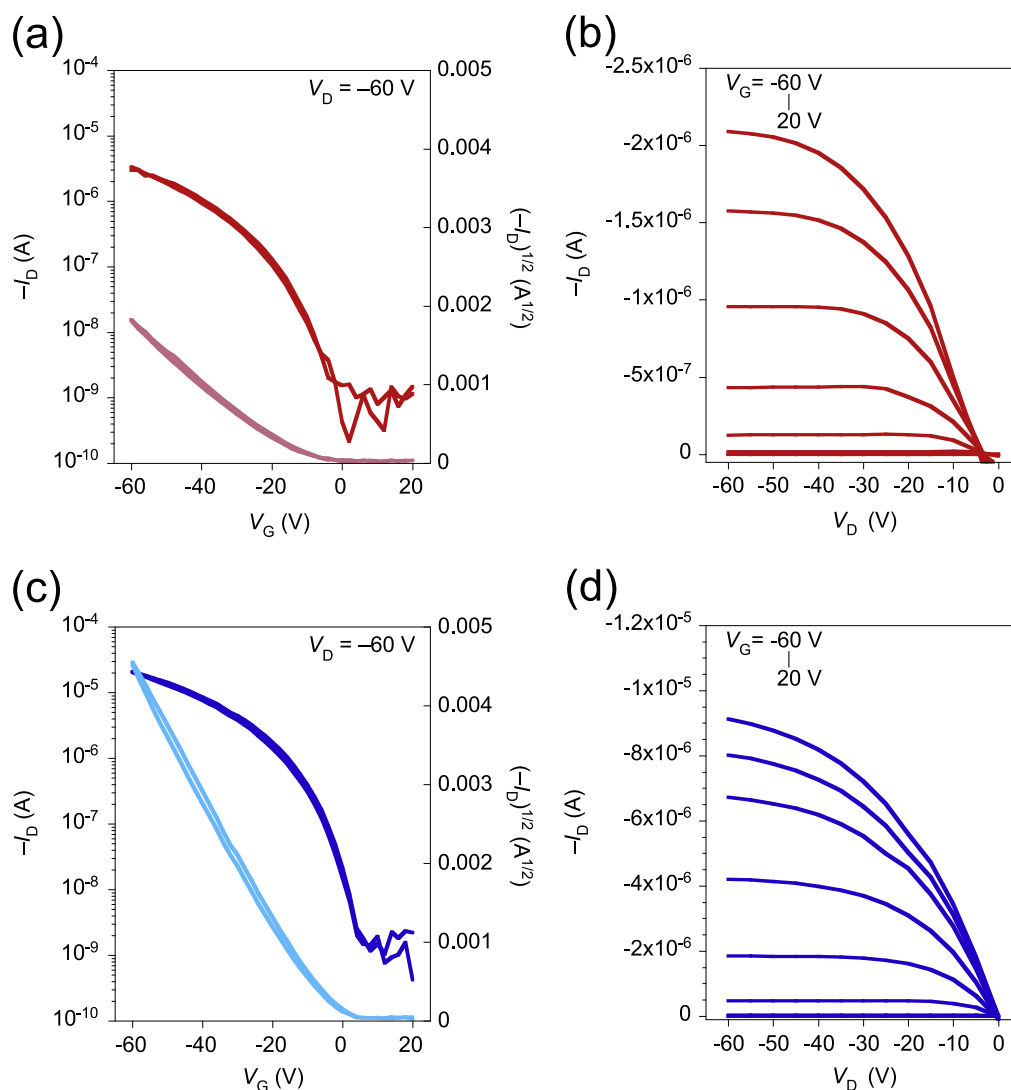
Figure 6. Transfer curves (a), (c) and output curves (b), (d) of the OFET devices based on PNDT3iBT (a), (b) and PNDT4iBT (c), (d).

than that of PNDT3BT (the more red-shifted one in PNDTBTs), the absorption edge (λ_{edge}) reached ca. 590 nm, corresponding to the energy gap E_g of 2.17 eV, which is almost the same as that for PNDT3BT (2.15 eV). From these optical aspects, the NDT4 unit, when linked at the 5, 10-positions, is expected as a good building unit comparable to the NDT3 unit with the 2, 7-linkage, which would afford high-performance semiconducting polymers for OFETs and OPVs.

To further confirm the structural difference between PNDT3iBT and PNDT4iBT expected from the optical measurements, grazing incidence x-ray diffraction (GIXD) measurements were performed using the thin films. Figure 5 depicts the two-dimensional GIXD images and the cross-sections along the $\sim q_z$ and q_{xy} axes. Both PNDT3iBT and PNDT4iBT afforded textures assignable to the edge-on orientation, where the diffractions corresponding to the lamellar structure and the π–π stacking structure appeared along the $\sim q_z$ and q_{xy} axes, respectively (figure 5(a), (b)). However, the weaker π–π stacking diffraction of PNDTiBTs compared to that of PNDTBTs indicates a less ordered

structure. Although both polymers showed the lamellar diffractions up to the fourth order and the lamellar d-spacing (d_l) of 25.3 Å ($q_z = 0.25$ Å^{-1}), PNDT4iBT had the more intense peak and the narrower distance ($d\pi$) of 3.7 Å ($q_{xy} = 1.73$ Å) corresponding to the π–π stacking diffraction than PNDT3iBT ($d\pi = 3.9$ Å, $q_{xy} = 1.68$ Å^{-1}). This indicates that PNDT4iBT forms a structure with better crystallinity than PNDT3iBT does. Although the π–π stacking diffractions in PNDTiBTs were less prominent compared to those in PNDTBTs (figure 5(c), (d)), particularly PNDT4iBT had relatively narrow $d\pi$, despite the somewhat twisted backbone, which is likely attributed to the strong interaction of the NDT cores. In PNDTBTs, PNDT3BT showed more ordered peaks for the lamellar diffraction than PNDT4BT, suggesting that the crystallinity of PNDT3BT is higher. The contrasting trend in the ordering structure between PNDTBTs and PNDTiBTs is fairly consistent with the result of UV–vis absorption spectra.

OFET properties of the polymers were evaluated with bottom-gate top-contact devices, in which the Si/SiO$_2$ substrate was treated with 1H,1H,2H,2H-perfluorodecyltriethoxysilane (FDTS) and then the polymer

solution was spin-coated and annealed at 150 °C. Figure 6 displays the current–voltage characteristics of the OFETs. The maximum hole mobilities extracted from the saturation region were $0.0023\ cm^2\ V^{-1}\ s^{-1}$ for PNDT3iBT and $0.011\ cm^2\ V^{-1}\ s^{-1}$ for PNDT4iBT, respectively. The higher mobility in PNDT4iBT than in PNDT3iBT is quite reasonable considering the difference in crystallinity as described above.

4. Conclusions

We presented new semiconducting polymers with NDT cores linked at the naphthalene positions. It is interesting that the linking fashion drastically changed the trend in the ordering structure, and the charge transport properties. As previously reported, when the NDT cores are linked at the thiophene α-positions, the NDT3-based polymer gave the better ordering in thin films and thus the high charge carrier mobility compared to the NDT4-based polymer. However, when NDTs are linked at the naphthalene positions, due to the steric hindrance between the C-H moieties on the NDT core and on neighboring thiophenes, the backbone of the NDT3-based polymer (PNDT3iBT) was more twisted than the NDT4-based polymer (PNDT4iBT), which gave rise to the lesser ordered structure and thus the lower charge carrier mobility. Considering the fact that PNDT4iBT has a relatively low HOMO level of $-5.2\ eV$ and moderately high mobilities in the order of $10^{-2}\ cm^2\ V^{-1}\ s^{-1}$, the NDT4 core, when linked at the naphthalene positions, can be a good building unit for the development of high-performance semiconducting polymers for OFETs and OPVs.

References

[1] Beaujuge P M and Fréchet J M J 2011 *J. Am. Chem. Soc.* **133** 20009
[2] Facchetti A 2011 *Chem. Mater.* **23** 733
[3] McCulloch I, Heeney M, Bailey C, Genevicius K, MacDonald I, Shkunov M, Sparrowe D, Tierney S, Wagner R and Zhang W 2006 *Nature Mater.* **5** 328
[4] Li Y, Wu Y, Liu P, Birau M, Pan H and Ong B 2006 *Adv. Mater.* **18** 3029
[5] Pan H, Li Y, Wu Y, Liu P, Ong B S, Zhu S and Xu G 2007 *J. Am. Chem. Soc.* **129** 4112
[6] Pan H, Wu Y, Li Y, Liu P, Ong B S, Zhu S and Xu G 2007 *Adv. Funct. Mater.* **17** 3574
[7] Rieger R, Beckmann D, Pisula W, Steffen W, Kastler M and Müllen K 2010 *Adv. Mater.* **22** 83
[8] Li J, Qin F, Li C M, Bao Q, Chan-Park M B, Zhang W, Qin J and Ong B S 2008 *Chem. Mater.* **20** 2057
[9] Fong H H, Pozdin V A, Amassian A, Malliaras G G, Smilgies D-M, He M, Gasper S, Zhang F and Sorensen M 2008 *J. Am. Chem. Soc.* **130** 13202
[10] Nakano M, Osaka I, Takimiya K and Koganezawa T 2014 *J. Mater. Chem. C* **2** 64
[11] Osaka I, Abe T, Shinamura S, Miyazaki E and Takimiya K *J. Am. Chem. Soc.* 2010 **132** 5000
[12] Osaka I, Abe T, Shinamura S and Takimiya K 2011 *J. Am. Chem. Soc.* **133** 6852
[13] Osaka I, Shinamura S, Abe T and Takimiya K 2013 *J. Mater. Chem. C* **1** 1297
[14] Osaka I, Abe T, Shimawaki M, Koganezawa T and Takimiya K 2012 *ACS Macro Lett.* **1** 437
[15] Osaka I, Kakara T, Takemura N, Koganezawa T and Takimiya K 2013 *J. Am. Chem. Soc.* **135** 8834
[16] Loser S, Miyauchi H, Hennek J W, Smith J, Huang C, Facchetti A and Marks T J 2012 *Chem. Commun.* **48** 8511
[17] Shi S, Jiang P, Yu S, Wang L, Wang X, Wang M, Wang H, Li Y and Li X 2013 *J. Mater. Chem. A* **1** 1540
[18] Shi S, Xie X, Jiang P, Chen S, Wang L, Wang M, Wang H, Li X, Yu G and Li Y 2013 *Macromolecules* **46** 3358
[19] Cheng S-W, Chiou D-Y, Lai Y-Y, Yu R-H, Lee C-H and Cheng Y-J 2013 *Org. Lett.* **15** 5338
[20] Shinamura S, Sugimoto R, Yanai N, Takemura N, Kashiki T, Osaka I, Miyazaki E and Takimiya K 2012 *Org. Lett.* **14** 4718
[21] Shinamura S, Miyazaki E and Takimiya K 2010 *J. Org. Chem.* **75** 1228
[22] Shinamura S, Osaka I, Miyazaki E, Nakao A, Yamagishi M, Takeya J and Takimiya K 2011 *J. Am. Chem. Soc.* **133** 5024
[23] Ishiyama T, Takagi J, Ishida K, Miyaura N, Anastasi N R and Hartwig J F 2001 *J. Am. Chem. Soc.* **124** 390